NUMERICAL ANALYSIS OF THE MECHANICAL BEHAVIOR OF A TUNNEL EXCAVATED IN SWELLING ROCKMASS

Xiaodong LIU[1*], Seishiro MATSUBARA[1], Shotaro YAMADA[1], Takashi KYOYA[1]

[1] Dept. of Civil Eng., Tohoku University
(Aramaki Aza-Aoba 6-6-06, Aoba-ku, Sendai 980-8579, Japan)
*E-mail: liu.xiaodong.r5@dc.tohoku.ac.jp

1. INTRODUCTION

In recent years, a problem that ground expansion by swelling clay minerals destroys the roadbed of a mountainous tunnel has occurred in various regions in Japan. The heave of tunnel invert caused by swellable minerals will seriously affect the normal operation and endanger the structural safety of the tunnel, and therefore, it is very important to make appropriate predictions of the mechanical behavior of the tunnel for the support system design and maintenance.

The expansion comes with the process of water-absorption between layers of these clay minerals[1)]. In addition, it is reported that the hygroscopic expansion, which is based on a thermo-chemical phenomenon, degrades the stiffness of the ground as the swelling clay minerals interact with surrounding intact rock[2)]. The complicated mechanical behavior of the ground involving swelling clay minerals comes from a kind of phenomena based on multi-physics, due to the hygroscopic expansion. Although it should be to simulate the complicated behavior theoretically in terms of multi-scale/multi-physics analysis which considered the thermo-mechanics with chemical reactions, no applicable model has yet to be developed in practice.

From a viewpoint of engineering practice, the purpose of this study is to construct a numerical analysis method to estimate the stress state and deformation of a tunnel during the process of excavation and hygroscopic expansion. And it is acknowledged that the accuracy and robustness of the finite element method (FEM) program can be improved by the implicit integration algorithm, especially when complex elastoplastic constitutive models are used[3)]. Therefore, the present study formulates the return mapping algorithm for the swell model based on MCC model, which is a constitutive model that can perform the softening and hardening behavior of ground material[4)].

2. PROCESS OF ANALYSIS

In this study, the three-stage analyses will be conducted, which contains initial stress field analysis, excavation analysis and swelling analysis, to obtain the stress-strain distribution characteristics of the tunnel in the process of expansion by water-absorption after excavation.

(1) Initial stress field analysis

Although the initial stress field of the mountains is very complex as it is affected by various factors such as self-weight, tectonic movement, geothermal field and so on, it will be computed only taking self-weight into consideration in this study as an initial pilot study. And the complex initial stress field can be achieved by applying different boundary conditions if other factors are considered such as tectonic movement.

(2) Excavation analysis

The excavation process of tunnel will cause the redistribution of the stress filed. The excavation analysis is carried out by applying the equivalent excavation load at the excavation boundary.

(3) Swelling analysis

In this study, the swelling elastoplastic constitutive model is established by introducing the swelling strain, which is based on modified Cam-Clay model. And the formulation is presented in the next section.

3. FORMULATION OF SWELLING MODEL

(1) Basic equations

The strain is defined by three part as follows, swelling strain $\boldsymbol{\varepsilon}^{swe}$ is considered as non-mechanical strain.

$$\boldsymbol{\varepsilon} = \boldsymbol{\varepsilon}^{e} + \boldsymbol{\varepsilon}^{p} + \boldsymbol{\varepsilon}^{swe} \tag{1}$$

Where the upper index e and p are meant elastic and plastic parts of strain respectively. So the elastic constitutive relation can be written as:

$$\boldsymbol{\sigma}' = \boldsymbol{C}(\boldsymbol{\varepsilon} - \boldsymbol{\varepsilon}^{p} - \boldsymbol{\varepsilon}^{swe}) \tag{2}$$

$\boldsymbol{\sigma}'$ is the effective stress tensor, $\boldsymbol{C}$ is the elastic modules tensor. The yield function is the same as the Modified Cam-Clay model, given by

$$f(\boldsymbol{\sigma}',\alpha) = \mathrm{MD}\left[\ln\left(\frac{\mathrm{M}^2 + (\mathrm{q}/\mathrm{p}')^2}{\mathrm{M}^2}\right) + \ln\left(\frac{\mathrm{p}'}{\mathrm{p}'_\mathrm{c}}\right)\right] - \alpha \tag{3}$$

Where

$$\mathrm{p}' = \frac{1}{3}\mathrm{tr}(\boldsymbol{\sigma}') \quad \text{and} \quad \mathrm{q} = \sqrt{\frac{3}{2}}\|\mathrm{dev}(\boldsymbol{\sigma}')\| \tag{4}$$

$$\mathrm{MD} = \frac{\tilde{\lambda} - \tilde{\kappa}}{(1+\mathrm{e}_0)} \quad \text{and} \quad \alpha = \varepsilon_\mathrm{v}^\mathrm{p} = \mathrm{tr}\,\boldsymbol{\varepsilon}^\mathrm{p} \tag{5}$$

p' is the mean effective stress, q is the equivalent stress, M is the critical state parameter, D is the dilatancy coefficient, $\tilde{\lambda}$ is the compression index, $\tilde{\kappa}$ is the swelling index, e_0 is the initial void ratio corresponding to preconsolidation stress p'_c; α is a hardening parameter defined by plastic volumetric strain $\varepsilon_\mathrm{v}^\mathrm{p}$. By applying associated flow rule, the plastic strain rate is expressed as

$$\dot{\boldsymbol{\varepsilon}}^{p} = \gamma\frac{\partial f}{\partial \boldsymbol{\sigma}} \tag{6}$$

Where $\partial f / \partial \boldsymbol{\sigma}$ is the gradient of yield function f, which describe the directions of plastic strain increment. And plastic strain rate $\dot{\boldsymbol{\varepsilon}}^{p}$ can be decomposed into a spherical and deviatoric parts as follows.

$$\dot{\varepsilon}_v^p = \gamma\frac{\partial f}{\partial p'} \quad and \quad \dot{\varepsilon}_s^p = \gamma\frac{\partial f}{\partial q} \tag{7}$$

(2) Return Mapping algorithm

The backward Euler method is used to update the internal state variables and stress implicitly at local iterative algorithm. The backward Euler approximation is used for both the elastic properties and hardening rule, but the hard parameter α has explicit relation with plastic strain as equation (5), so the residual of backward Euler equations can be written as follows:

$$\mathbf{R}_{\mathrm{n+1}}^{\mathrm{f}} = -\boldsymbol{\varepsilon}_{\mathrm{n+1}}^{\mathrm{p}} + \boldsymbol{\varepsilon}_{\mathrm{n}}^{\mathrm{p}} + \Delta\gamma_{\mathrm{n+1}}\frac{\partial f_{\mathrm{n+1}}}{\partial \boldsymbol{\sigma}'} \tag{8}$$

$$\mathrm{R}_{\mathrm{n+1}}^{\mathrm{y}} = f(\boldsymbol{\sigma}'_{\mathrm{n+1}}, \alpha_{\mathrm{n+1}}) \tag{9}$$

Taking $\boldsymbol{\varepsilon}^\mathrm{p}, \alpha, \Delta\gamma$ as the main variable, and $\boldsymbol{\sigma}'$ as the Dependent variable, the linearization of the above equations are

$$\mathbf{R}_{\mathrm{n+1}}^{\mathrm{f}} + \left.\frac{\partial \mathbf{R}_{\mathrm{n+1}}^{\mathrm{f}}}{\partial \boldsymbol{\varepsilon}_{\mathrm{n+1}}^{\mathrm{p}}}\right|^{(\mathrm{k})} \delta\boldsymbol{\varepsilon}^{\mathrm{p}} + \left.\frac{\partial \mathbf{R}_{\mathrm{n+1}}^{\mathrm{f}}}{\partial \alpha_{\mathrm{n+1}}}\right|^{(\mathrm{k})} \delta\alpha + \left.\frac{\partial \mathbf{R}_{\mathrm{n+1}}^{\mathrm{f}}}{\partial (\Delta\gamma_{\mathrm{n+1}})}\right|^{(\mathrm{k})} \delta(\Delta\gamma) = \mathbf{0} \tag{10}$$

$$\mathrm{R}_{\mathrm{n+1}}^{\mathrm{y}} + \left.\frac{\partial f_{\mathrm{n+1}}}{\partial \boldsymbol{\varepsilon}_{\mathrm{n+1}}^{\mathrm{p}}}\right|^{(\mathrm{k})} : \delta\boldsymbol{\varepsilon}^{\mathrm{p}} + \left.\frac{\partial f_{\mathrm{n+1}}}{\partial \alpha_{\mathrm{n+1}}}\right|^{(\mathrm{k})} \delta\alpha = 0 \tag{11}$$

The (k) means the value the coefficient at the k-th iteration during the analysis step in $[\mathrm{t}_\mathrm{n}, \mathrm{t}_{\mathrm{n+1}}]$. Solving the equation (10) and (11) about the correction of the main variable $\Delta\gamma$ and $\boldsymbol{\varepsilon}^\mathrm{p}$, and the corrections can be solved as follows:

$$\delta(\Delta\gamma) = \frac{f_{\mathrm{n+1}} - \boldsymbol{\Xi}_\mathrm{B} : \boldsymbol{\Xi}_\mathrm{A}\mathbf{R}_{\mathrm{n+1}}^{\mathrm{f}}}{\boldsymbol{\Xi}_\mathrm{B} : \boldsymbol{\Xi}_\mathrm{A}\dfrac{\partial f_{\mathrm{n+1}}}{\partial \boldsymbol{\sigma}'}} \tag{12}$$

$$\delta\boldsymbol{\varepsilon}^{\mathrm{p}} = -\boldsymbol{\Xi}_\mathrm{A}\left[\mathbf{R}_{\mathrm{n+1}}^{\mathrm{f}} + \frac{\partial f_{\mathrm{n+1}}}{\partial \boldsymbol{\sigma}'}\delta(\Delta\gamma)\right] \tag{13}$$

Where

$$\boldsymbol{\Xi}_\mathrm{A} = \left[-\mathbf{I}_{(4)} - \Delta\gamma_{\mathrm{n+1}}\frac{\partial^2 f_{\mathrm{n+1}}}{\partial \boldsymbol{\sigma}'^2_{\mathrm{n+1}}}\mathbf{C}\right]^{-1} \tag{14}$$

$$\boldsymbol{\Xi}_\mathrm{B} = \left[-\frac{\partial f_{\mathrm{n+1}}}{\partial \boldsymbol{\sigma}'_{\mathrm{n+1}}}\mathbf{C} - \mathbf{I}_{(2)}\right] \tag{15}$$

Using equation (5), the correction of hard parameter can be obtained:

$$\delta\alpha = \mathbf{I}_{(2)} : \delta\boldsymbol{\varepsilon}_{\mathrm{n+1}}^{\mathrm{p}} \tag{16}$$

And then we can update state variables as follows:

$$\begin{aligned} \Delta\gamma_{\mathrm{n+1}}^{(\mathrm{k+1})} &= \Delta\gamma_{\mathrm{n+1}}^{(\mathrm{k})} + \delta\gamma \\ \boldsymbol{\varepsilon}_{\mathrm{n+1}}^{\mathrm{p(k+1)}} &= \boldsymbol{\varepsilon}_{\mathrm{n+1}}^{\mathrm{p(k)}} + \delta\boldsymbol{\varepsilon}^{\mathrm{p}} \\ \alpha_{\mathrm{n+1}}^{(\mathrm{k+1})} &= \alpha_{\mathrm{n+1}}^{(\mathrm{k})} + \delta\alpha \end{aligned} \tag{17}$$

(3) Consistent tangent moduli

The consistent tangent operator can increase the rate of convergence significantly relative to the continuum tangent operator, and it can make the solution converged quadratically in full Newton-Raphson iteration when a non-linear constitutive model analyzed in FEM[5]. Differentiating equations (6), (2), (3) results in:

$$\mathrm{d}\boldsymbol{\varepsilon}_{\mathrm{n+1}}^{\mathrm{p}} = \frac{\partial f_{\mathrm{n+1}}}{\partial \boldsymbol{\sigma}'}\mathrm{d}(\Delta\gamma_{\mathrm{n+1}}) + \Delta\gamma_{\mathrm{n+1}}\frac{\partial^2 f_{\mathrm{n+1}}}{\partial \boldsymbol{\sigma}'^2}\mathrm{d}\boldsymbol{\sigma}_{\mathrm{n+1}} \tag{18}$$

$$\mathrm{d}\boldsymbol{\sigma}'_{\mathrm{n+1}} = \mathbf{C}\,\mathrm{d}\left(\boldsymbol{\varepsilon}_{\mathrm{n+1}} - \boldsymbol{\varepsilon}_{\mathrm{n+1}}^{\mathrm{p}} - \boldsymbol{\varepsilon}_{\mathrm{n+1}}^{\mathrm{swe}}\right) = \mathbf{C}\,\mathrm{d}\left(\boldsymbol{\varepsilon}_{\mathrm{n+1}} - \boldsymbol{\varepsilon}_{\mathrm{n+1}}^{\mathrm{p}}\right) \tag{19}$$

$$\mathrm{d}f(\boldsymbol{\sigma}_{\mathrm{n+1}}, \alpha_{\mathrm{n+1}}) = \frac{\partial f_{\mathrm{n+1}}}{\partial \boldsymbol{\sigma}'_{\mathrm{n+1}}} : \mathrm{d}\boldsymbol{\sigma}'_{\mathrm{n+1}} + \frac{\partial f_{\mathrm{n+1}}}{\partial \alpha_{\mathrm{n+1}}}\mathrm{d}\alpha_{\mathrm{n+1}} \tag{20}$$

Solving the equations above to get the relation between $d\boldsymbol{\sigma}'_{n+1}$ and $d\boldsymbol{\varepsilon}_{n+1}$, which is the algorithm consistent tangent moduli.

$$d\boldsymbol{\sigma}'_{n+1} = \left[\boldsymbol{\Xi}_{n+1} - \frac{\boldsymbol{\Xi}_{n+1} \dfrac{\partial f_{n+1}}{\partial \boldsymbol{\sigma}'} \otimes \boldsymbol{\Xi}_{n+1} \boldsymbol{\eta}_{n+1}}{\left(\mathbf{I}_{(2)} : \dfrac{\partial f_{n+1}}{\partial \boldsymbol{\sigma}'} \right) + \boldsymbol{\eta}_{n+1} : \left(\boldsymbol{\Xi}_{n+1} \dfrac{\partial f_{n+1}}{\partial \boldsymbol{\sigma}'} \right)} \right] d\boldsymbol{\varepsilon}_{n+1} \tag{21}$$

Where

$$\boldsymbol{\Xi}_{n+1} = \left[\mathbf{C}_{n+1}^{-1} + \Delta\gamma_{n+1} \frac{\partial^2 f_{n+1}}{\partial \boldsymbol{\sigma}'^2} \right]^{-1} \tag{22}$$

$$\boldsymbol{\eta}_{n+1} = \left[\frac{\partial f_{n+1}}{\partial \boldsymbol{\sigma}'} - \Delta\gamma_{n+1} \frac{\partial^2 f_{n+1}}{\partial \boldsymbol{\sigma}'^2} \mathbf{I}_{(2)} \right] \tag{23}$$

4. EXAMPLE OF ANALYSIS

The simulation of a tunnel constructed in swelling rockmass is carried out using the analysis method presented in section 2 and 3. The parameters used for analysis are shown in **Table 1**.

Table 1 Parameters used in presented model.

E (GPa)	p'_c (MPa)	M	$\tilde{\lambda}$	$\tilde{\kappa}$	υ	e_0
3	100	1.0	0.25	0.05	0.3	1.0

(1) Initial stress analysis

The model of **Fig.1** shows the boundary conditions and cross-section of the tunnel for initial stress analysis. $\boldsymbol{\sigma}_v$ is set as $88\,\mathrm{kN/m^2}$ and the initial mean effective stress is shown in **Fig.2** .

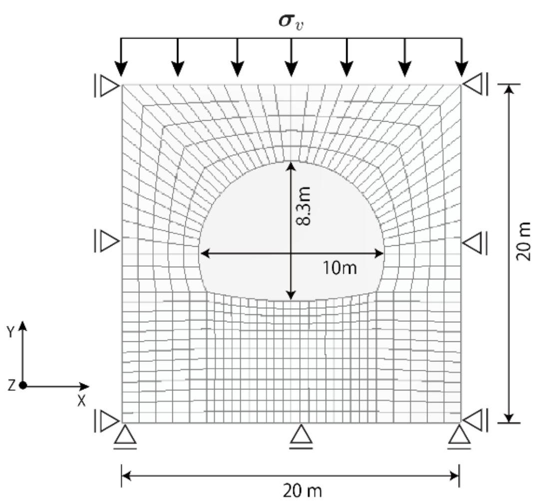

Fig.1 Model for initial stress analysis

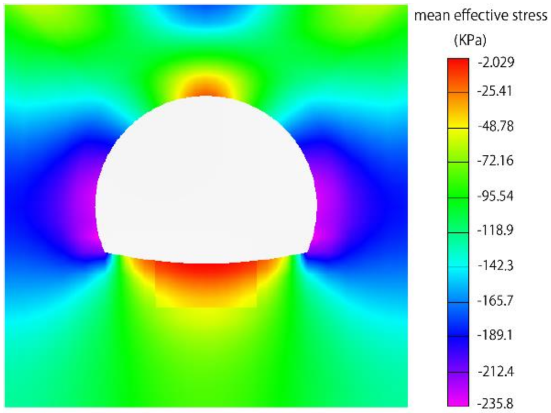

Fig.2 Initial stress state

(2) Swelling analysis

The model for swelling analysis is shown in **Fig.3**. The yellow domain is set as the swelling part with the total swelling strain $\varepsilon^{swe} = 10\%$ which is divided into 500 steps in FEM analysis.

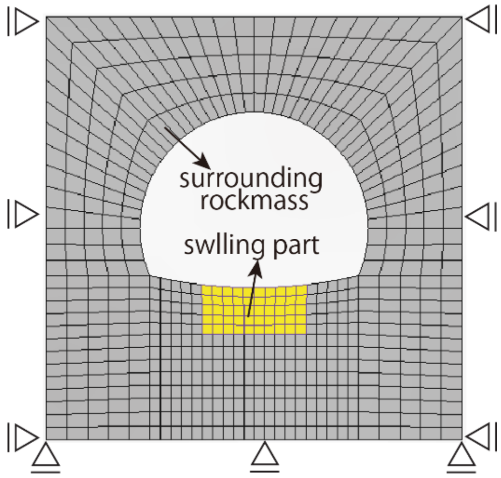

Fig.3 Model for swelling analysis

Swelling simulation is conducted from the stress state computed in initial stress analysis. The displacement and equivalent stress distribution are shown in **Fig.4** and **Fig.5**. The max displacement is about 0.974m in the end of swelling process. The P'-q stress path of the check point shown in **Fig.5** is shown in **Fig.6**. The stress path illustrates the swelling pressure increases when swelling process occurs in the elastic stage and it decreases in the plastic stage because of the plastic volume expansion over the critical state line.

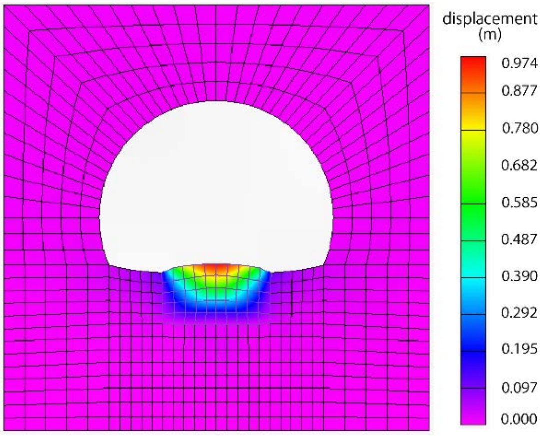

Fig.4 Displacement distribution

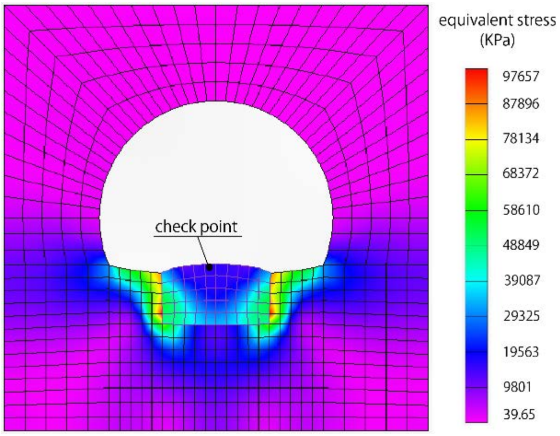

Fig.5 Equivalent stress distribution

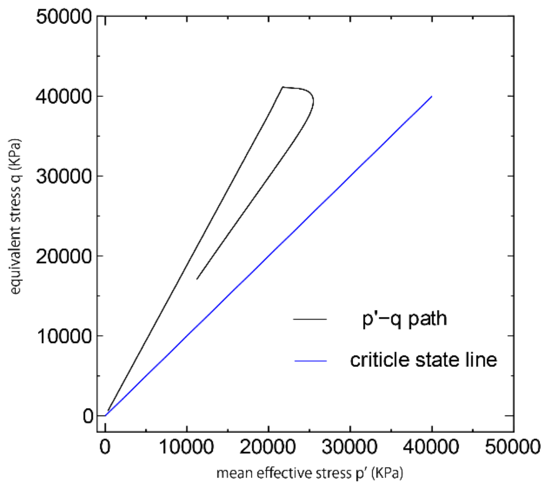

Fig.6 Stress path of swelling process

5. CONCLUTION AND DISCUSSION

An elasto-plastic swell model based on MCC is proposed in this study. And the formulation of return mapping algorithm is effective verified by some numerical examples. The proposal model made it possible to evaluate displacement and stress state of the tunnel roadbed. Of course, it is still insufficient to evaluate the mechanical behavior of the tunnels constructed in swelling rockmass accurately. We will modify the model for it is more applicable to the real problems.

REFERENCES

1) Grim, R.E., 1968, Clay Mineralogy, 2nd Ed, New York: McGraw Hill
2) Luc Massat, Olivier Cuisinier, Isabelle Bihannic et al., 2016, Swelling pressure development and inter-aggregate porosity evolution upon hydration of a compacted swelling clay, Applied Clay Science, 197-210.
3) Simo, J.C. and Hughes, T.J.R., 1998, Computational Inelasticity. New York: Springer
4) Schofield, A. and Wroth, P., 1968, Critical State Soil Mechanics. Lecturers in Engineering at Cambridge University. London: McGraw Hill.
5) Simo, J.C., and Taylor, R.L., 1985, Consistent Tangent Operator for Rate-lndependent Elastoplasticity. Computer Meth. in Applied Mech. and Eng. Vol.48, 101-118.